[CANCER RESEARCH 55, 4824–4829, November 1, 1995]

Advances in Brief

Tumor Necrosis Factor α-induced Leukocyte Adhesion in Normal and Tumor Vessels: Effect of Tumor Type, Transplantation Site, and Host Strain[1]

Dai Fukumura,[2] Hassan A. Salehi,[2] Brian Witwer, Ronald F. Tuma, Robert J. Melder, and Rakesh K. Jain

Edwin L. Steele Laboratory, Department of Radiation Oncology, Massachusetts General Hospital and Harvard Medical School, Boston, Massachusetts 02114 [D. F., H. A. S., B. W., R. J. M., R. K. J.], and Departments of Physiology and Neurosurgery, Temple University School of Medicine, Philadelphia, Pennsylvania 19140 [R. F. T.]

Abstract

Tumor necrosis factor α (TNF-α) can lead to tumor regression when injected locally or when used in an isolated limb perfusion, and it can enhance the tumoricidal effect of various therapies. TNF-α can also up-regulate adhesion molecules and, thus, facilitate the binding of leukocytes to normal vessels. The present study was designed to investigate the extent to which the host leukocytes roll and adhere to vessels of different tumors (MCaIV, a murine mammary adenocarcinoma; HGL21, a human malignant astrocytoma) at a given site or to the same tumor at different sites (dorsal skin and cranium), in different mouse strains [C3H and severe combined immunodeficient (SCID)], both with and without TNF-α-activation. There was no significant difference in hemodynamic parameters such as RBC velocity, diameter, or shear rate between PBS-treated control groups and corresponding TNF-α-treated groups. Under PBS control conditions, the leukocyte rolling count in MCaIV tumor vessels in the dorsal chamber in C3H and SCID mice and in the cranial window in C3H mice was significantly lower than that in normal vessels ($P < 0.05$), but stable cell adhesion was similar between normal and tumor vessels. TNF-α led to an increase ($P < 0.05$) in leukocyte-endothelial interaction in vessels in the following cases: normal tissue regardless of sites and strains, MCaIV tumor in the dorsal chamber in C3H and SCID mice, MCaIV tumor in the cranial window in C3H mice, and HGL21 tumor in the cranial window in SCID mice. However, the increase in rolling and adhesion in the MCaIV tumor in response to TNF-α was significantly lower than in the corresponding normal vessels ($P < 0.05$) in the dorsal chamber in C3H and SCID mice and in the cranial window in C3H mice. The HGL21 tumor in the cranial window in SCID mice showed leukocyte rolling and adhesion comparable to that in normal pial vessels. These findings suggest that (*a*) in general, basal leukocyte rolling is lower in tumor vessels than in normal vessels; (*b*) leukocyte rolling and adhesion in tumors can be enhanced by TNF-α-mediated activation; and (*c*) the TNF-α response is dependent on tumor type, transplantation site, and host strain. These results have significant implications in the gene therapy of cancer using TNF-α-gene-transfected cancer cells or lymphocytes.

Introduction

Systemic injection of TNF-α[3] can lead to severe toxicity including fever, nausea, loss of appetite, fatigue, lassitude, and hypotension (1, 2). On the other hand, when injected locally or used in isolated limb perfusion, TNF-α can lead to tumor regression (2). TNF-α can also enhance the tumoricidal effect of natural killer cells, ionizing radiation, and hyperthermia (3–6). TNF-α can also improve radio-antibody uptake in human colon carcinoma xenografts by increasing vascular permeability (7). Finally, TNF-α can up-regulate the adhesion molecules such as E and P selectins, ICAM-1, and VCAM-1, and, thus, facilitates binding of leukocytes to normal vessels (8, 9). However, the extent to which leukocytes adhere to these molecules in TNF-α-activated vessels of different tumors at a given site or the same tumor at different sites is not known.

Wu *et al.* (10) using a rat dorsal skin chamber and a rat mammary tumor (R3230AC) showed that the adhesion of leukocytes both under normal conditions and after activation by formylmethionylleucylphenylalanine, lipopolysaccaride, and TNF-α is lower in the tumor microvasculature compared to the normal tissue vessels. Ohkubo *et al.* (11), on the other hand, using a rabbit ear chamber and a VX2 carcinoma model showed that IL-2 increases the rolling of leukocytes in the tumor vessels more than in host vessels. Sasaki *et al.* (12) showed preferential adhesion of adoptively transferred human A-NK cells to the rabbit VX2 carcinoma vessels. Melder *et al.* (13, 14) using positron emission tomography and intravital microscopy, showed preferential adhesion of syngeneic IL-2-activated A-NK cells in two different murine tumors, FSaII and MCaIV. Mechanisms of these differences in the relative degree of leukocyte adhesion to the tumor and normal microvasculature are not known. In the present study, we test the hypothesis that leukocyte-endothelial interaction depends on tumor type, transplantation site, and host strain.

Materials and Methods

Animals, Surgery, and Tumor Implantation. Dorsal skin chambers (15) and cranial windows (16) were implanted in mice by using the procedure described elsewhere. Two-month-old C3H and SCID mice (25–30 g) were used. A 1-mm diameter fragment of MCaIV (a murine mammary adenocarcinoma) or HGL21 (human glioblastoma) was implanted in the center of the dorsal or cranial window. MCaIV was grown in the dorsal and cranial windows in C3H and SCID mice. HGL21 was grown only in the cranial window in SCID mice because it does not grow in the dorsal skin chamber. The measurements were made between days 8 and 9 for MCaIV and between days 12 and 14 for HGL21 when the tumor occupied about one-half of the window surface area. None of the tumor implants were rejected by the host.

Tracer and Growth Factor. TNF-α (Cetus/Chiron, Emeryville, CA) was diluted to a final concentration of 100 ng/10 μl, FITC-labeled dextran (M_r, 2,000,000; 50 mg/ml; Sigma Chemical Co., St. Louis, MO) to 1%, and Rho-6G (Molecular Probes, Eugene, OR) to 0.1%. The FITC and Rho-6G solutions were passed through a 0.2-μm filter before injection.

Experimental Procedure. For baseline measurements without any treatment, the coverslip was left intact. For treatment with 1× PBS (Sigma) or TNF-α, the coverslip was removed, and 20 μl of either PBS or TNF-α was applied to the normal or tumor tissue surface for 15 min and covered with a cover glass again. Four h later, the animals were anesthetized with a cocktail of Ketamine (Ketalar, Parke-Davis, Morris Plains, NJ) and Xylazine (Fermenta, Kansas City, MO), 90 and 9 mg/kg, respectively, s. c. The mice were then placed under an intravital fluorescence microscope (Axioplan; Zeiss, Oberkochen, Germany) equipped with the fluorescence filter set for Rho-6G and FITC (Omega Optical, Inc., Brattleboro, VT), an intensified CCD video camera (C2400–88; Hamamatsu Photonics K.K., Hamamatsu, Japan), a CCD video camera (AVC-D7; Sony, Tokyo, Japan), and a S-VHS videocassette recorder (SVO-9500MD; Sony).

Received 7/24/95; accepted 8/28/95.

The costs of publication of this article were defrayed in part by the payment of page charges. This article must therefore be hereby marked *advertisement* in accordance with 18 U.S.C. Section 1734 solely to indicate this fact.

[1] This work was supported by an American Cancer Society grant (to R. K. J.). D. F. is a DuPont Merck Fellow.

[2] Authors contributed equally to this paper.

[3] The abbreviations used are: TNF-α, tumor necrosis factor α; A-NK, lymphokine-activated natural killer; SCID, severe combined immunodeficient; Rho-6G, rhodamine 6G; CCD, charge coupled device; IL-2, interleukin 2.

Downloaded from http://aacrjournals.org/cancerres/article-pdf/55/21/4824/2459027/cr0550214824.pdf by guest on 24 August 2022

The four-slit technique was used to measure the RBC velocity in tumor vessels and in normal postcapillary venules with diameters of about 20 μm. For the dorsal window, transillumination was used (15). For the cranial window, FITC-labeled dextran (M_r, 2,000,000; 0.1 ml/25 g body weight) was injected through the tail vein for contrast enhancement between RBCs and plasma (16). Five to eight vessels were chosen randomly from the periphery or the central region of the tumor or normal tissues. In each animal, video images of blood flow were recorded for 60 s. The vessels that had no flow were not included. The recordings were later analyzed by the four-slit apparatus (Microflow System, model 208C, video photometer version; IPM, San Diego, CA) equipped with a personal computer (IBM PS/2, 40SX; Computerland, Boston, MA). The diameter, in μm, of the vessels was measured by using an image-shearing device (digital video image-shearing monitor, model 908; IPM). For monitoring leukocytes, the mice were given injections with an i.v. bolus of 20 μl of 0.1% Rho-6G in 0.9% saline through the tail vein. Rho-6G is a nontoxic fluorescent dye that is taken up by circulating leukocytes (17). Leukocyte behavior was visualized by intensified CCD camera and recorded for a 30-s period for each vessel.

Analysis and Interpretation. Rolling was defined as a short-term interaction and slow movement along vessel wall [<50% of RBC velocity (V)]; adhesion was defined as stable binding at a certain position for more than a 30-s period. The procedure used for quantifying *in vivo* leukocyte interaction to vascular endothelium was based on the method of Atherton and Born (18). In brief, the number of rolling (NR) and adhering (NA) leukocytes was counted for 30 s along a 100-μm segment of a vessel. The total flux of cells for 30 s was also measured (NT). All measurements were done off-line. The leukocyte flux was normalized by the cross-section area of each microvessel as follows: leukocyte flux (cells/mm^2/s) = $10^6 \times NT/[\pi \times (D/2)^2 \times 30\ s]$. The ratio of rolling cells to total flux (rolling count) as an indicator of leukocyte rolling was calculated as follows: rolling count (%) = $100 \times NR/NT$. The density of adhering leukocytes (D) as an indicator of leukocyte adhesion to vessels was calculated as follows: D (cells/mm^2) = $10^6 \times NA/(\pi \times D \times 100\ \mu m)$. Shear rate was calculated for each vessel as: shear rate = $8\ V/D$.

Statistical Considerations. Dorsal chambers were implanted in 27 C3H and 25 SCID mice. These animals were divided into the following five groups of five animals of each type, except for the C3H group 1 (seven animals). Three groups of tumor-free animals were used to measure RBC velocity, diameter, leukocyte rolling and adhesion in closed chambers (group 1), open chambers treated with PBS (group 2), and open chambers treated with TNF-α (group 3), respectively. Two groups of animals bearing MCaIV tumor were used to measure these parameters in open chambers treated with PBS (group 4), and with TNF-α (group 5), respectively. Cranial windows were implanted in 20 (4 groups of 5 animals/group) C3H and 35 (7 groups of 5 animals/group) SCID mice. Two groups of tumor free animals were used to measure RBC velocity, diameter, leukocyte rolling and adhesion in open chamber treated with PBS (group 2), and open chambers treated with TNF-α (group 3), respectively. Two groups of animals bearing MCaIV tumor were used to measure these parameters in open chambers treated with PBS (group 4) and TNF-α (group 5), respectively. In addition to the above 4 groups of C3H and 4 groups of SCID mice, cranial windows were implanted in 1 group of tumor-free SCID mice in closed windows (group 1) and in 2 groups of SCID mice to grow HGL21 to study the effect of PBS (group 6) and TNF-α (group 7), respectively.

The data from these 21 groups of 107 animals were analyzed by using an ANOVA and the Fisher's *post hoc* test. All values are expressed as mean ± SD, and statistical significance was set at $P < 0.05$.

Results

Dorsal Skin Chamber Study. RBC velocity in normal dorsal skin vessels with the coverslip intact versus open chambers treated with PBS was 0.183 ± 0.033 *versus* 0.141 ± 0.029 mm/s in C3H and 0.199 ± 0.016 *versus* 0.183 ± 0.048 mm/s in SCID mice, respectively. The diameter of normal skin postcapillary venules with coverslip intact *versus* open chambers treated with PBS was 20.0 ± 6.9 *versus* 20.1 ± 4.0 μm in C3H and 15.8 ± 2.0 *versus* 16.7 ± 2.4 μm in SCID, respectively. The shear rates of normal skin vessels with coverslip intact and open chamber treated with PBS were 86.1 ± 23.7 *versus* 65.0 ± 25.7 s^{-1} in C3H and 105.0 ± 19.2 *versus* 93.1 ± 34.3 s^{-1} in SCID, respectively. The normalized leukocyte flux in normal skin vessels with coverslip intact *versus* open chambers treated with PBS was 2134 ± 1553 *versus* 934 ± 699 cells/mm^2/s in C3H and 1647 ± 816 *versus* 1425 ± 644 cells/mm^2/s in SCID, respectively. The leukocyte rolling count in normal skin vessels with coverslip intact *versus* open chambers treated with PBS was 60.0 ± 13.0 *versus* 63.3 ± 9.9% in C3H and 62.9 ± 7.2 *versus* 62.2 ± 6.4% in SCID, respectively. The adhesion density in normal skin vessels with coverslip intact *versus* open chambers treated with PBS was 49.0 ± 112.6 *versus* 136.7 ± 110.9 cells/mm^2 in C3H and 54.3 ± 37.0 *versus* 42.2 ± 48.0 cells/mm^2 in SCID, respectively. No significant difference was observed in the value of any parameter between untreated groups with the window closed and corresponding PBS-treated groups with open coverslips in both C3H and SCID mice. These results suggest that the superfusion procedure did not influence the results in the dorsal window.

In C3H mice, there was no significant difference in hemodynamic parameters between normal and MCaIV tumor vessels in both PBS- and TNF-α-treated groups. In SCID mice, the calculated shear rate in the tumor vessels was lower than in normal vessels in both PBS and TNF-α. There was no significant difference in hemodynamic parameters such as RBC velocity, diameter, or shear rate between PBS-treated groups and corresponding TNF-α-treated groups in all pairs (Fig. 1). There also was no statistically significant difference in leukocyte flux in any comparison (Fig. 2*A*).

Under the PBS control condition, the rolling count in tumor vessels was significantly lower than in the corresponding normal vessels in both types of mice (Fig. 2*B*). The adhesion density was low in both normal and tumor vessels regardless of strain (Fig. 2*C*). Despite the differences in rolling interactions, there was no statistical difference in stable adhesion between normal and MCaIV tumor vessels without TNF-α activation. In TNF-α-treated groups, both the leukocyte rolling count and adhesion density were significantly higher than in the corresponding PBS-treated groups in both normal skin and tumor regardless of animal types except for adhesion density in SCID MCaIV tumor (Fig. 2). However, both the leukocyte rolling count and adhesion density in tumor vessels in TNF-α-treated groups were significantly lower than in the corresponding normal vessels regardless of mouse strain (Fig. 2).

Cranial Window Study. RBC velocity in normal pial vessels in cranial window in SCID mice with the coverslip intact was higher than in open window with PBS treatments (>1 mm/s *versus* 0.410 ± 0.079 mm/s); whereas the diameter (24.1 ± 3.4 *versus* 20.5 ± 2.9 μm) was comparable. Number of rolling leukocytes in closed window and after PBS treatment along 100-μm segment was 0.95 ± 1.0 cells/30 s and 7.84 ± 4.8 cells/30 s, respectively. Adhesion density in closed window and after PBS treatment was 16.4 ± 18.9 cells/mm^2 and 79.8 ± 83.8 cells/mm^2, respectively. These results suggest that the superfusion procedure may decrease the RBC velocity and shear rate in pial vessels and, hence, may contribute to increased rolling and adhesion during PBS superfusion. In contrast, opening the window did not affect RBC velocity or leukocyte-endothelial interaction in tumor vessels (data not shown).

The RBC velocity in MCaIV and HGL21 tumor vessels was significantly lower than in the corresponding normal vessels regardless of strain (Fig. 3*A*). In C3H mice, the vessel diameter was comparable between normal and MCaIV tumor tissue (Fig. 3*B*). However, in SCID mice, the diameter of MCaIV tumor vessels was larger and that of HGL21 tumor vessel was smaller than the normal vessel diameter (Fig. 3*B*). As a result, the shear rate of MCaIV tumor vessels was significantly lower than that in normal vessels and in HGL21 tumor vessels in SCID mice (Fig. 3*C*). These differences were consistent

Downloaded from http://aacrjournals.org/cancerres/article-pdf/55/21/4824/2459027/cr0550214824.pdf by guest on 24 August 2022

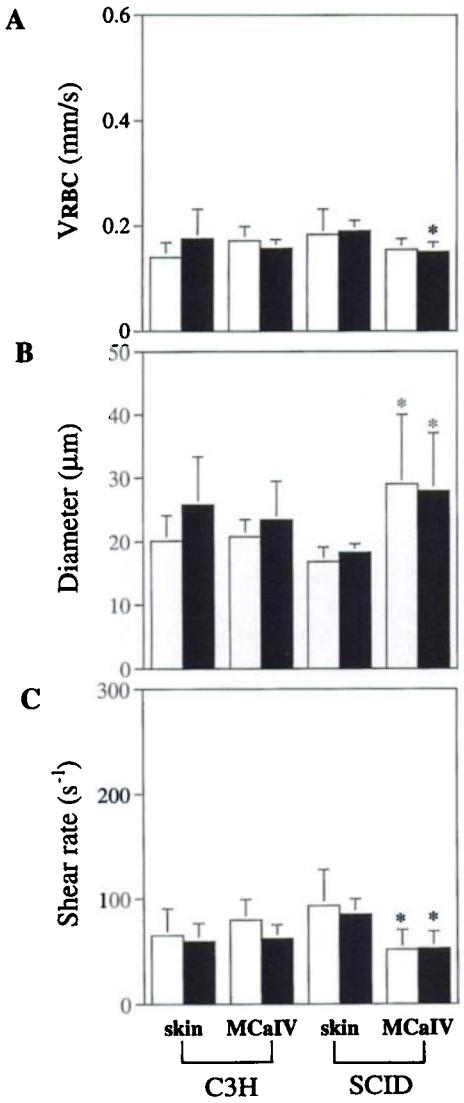

Fig. 1. Hemodynamic parameters in the dorsal skin chamber. *A*, RBC velocity (*V*); *B*, vessel diameters (*D*); *C*, calculated shear rates using *V* and *D* data in the dorsal skin chamber. □, PBS treatment groups; ■, TNF-α treatment groups. *Columns*, mean; *bars*, SD. *, a statistically significant difference ($P < 0.05$) as compared with corresponding value of normal skin vessels.

regardless of treatments. There was no significant difference in hemodynamic parameters between PBS-treated and corresponding TNF-α-treated groups in normal and tumor vessels (Fig. 3).

In SCID mice, leukocyte flux was significantly lower in both tumors treated with PBS and MCaIV tumor treated with TNF-α than corresponding normal tissues (Fig. 4*A*). In the remaining groups, there was no statistically significant difference in leukocyte flux.

Under the PBS control condition, the rolling leukocyte count in MCaIV tumor in C3H mice was significantly lower than in the corresponding normal vessels (Fig. 4*B*). However, in SCID mice, there was no significant difference in the rolling count in vessels of normal tissues and two tumors (Fig. 4*B*). There also was no significant difference in adhesion density between normal and tumor vessels regardless of the mouse strain (Fig. 4*C*).

The rolling leukocyte count of the TNF-α-treated group was significantly higher than the corresponding PBS treated group in the pial surface in normal C3H, in the MCaIV tumor in C3H mice and in the HGL21 tumor in SCID mice (Fig. 4*B*). The adhesion density of TNF-α-treated groups was significantly higher than in the PBS-treated groups in both pial circulation in normal C3H and SCID and MCaIV tumor in C3H mice (Fig. 4*C*). In the remaining groups the increase in rolling and adhesion was not statistically significant.

There was no significant difference in the rolling count between normal tissue and two different tumors in TNF-α-treated groups in both strains of mice (Fig. 4*B*). The adhesion density with TNF-α treatment in MCaIV tumor in C3H mice was significantly lower than the corresponding normal vessels (Fig. 4*C*). There was no significant difference in the density between normal and both types of tumor vessels in SCID mice (Fig. 4*C*)

Discussion

Our studies have demonstrated that the basal leukocyte rolling in the vasculature of two different tumors, the MCaIV breast adenocarcinoma and the HGL21 human astrocytoma, is significantly suppressed when compared to the normal vessels of the skin and pial surface. This observation suggests that the ability of circulating host leukocytes to interact with and recognize tumor vasculature is com-

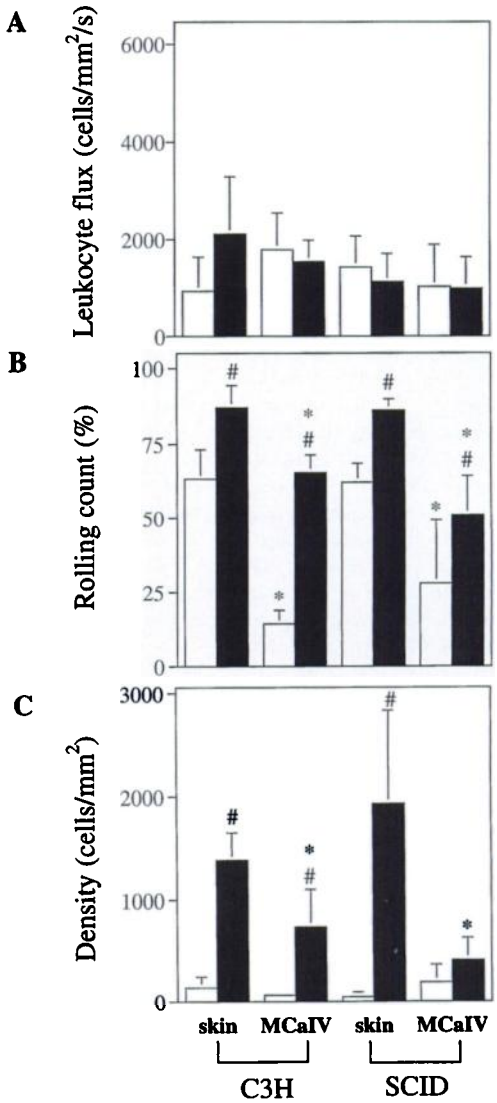

Fig. 2. Leukocyte-endothelial interaction in the dorsal skin chamber. *A*, normalized leukocyte flux; *B*, rolling count (100 × number of rolling cells/total number of cells) along 100-μm segment measuring for 30 s; *C*, density of binding cells. □, PBS treatment groups; ■, TNF-α treatment groups. *Columns*, mean; *bars*, SD. *, a statistically significant difference ($P < 0.05$) as compared with corresponding value of normal skin vessels. ≠, a statistically significant difference ($P < 0.05$) as compared with corresponding PBS control value.

Downloaded from http://aacrjournals.org/cancerres/article-pdf/55/21/4824/2459027/cr0550214824.pdf by guest on 24 August 2022

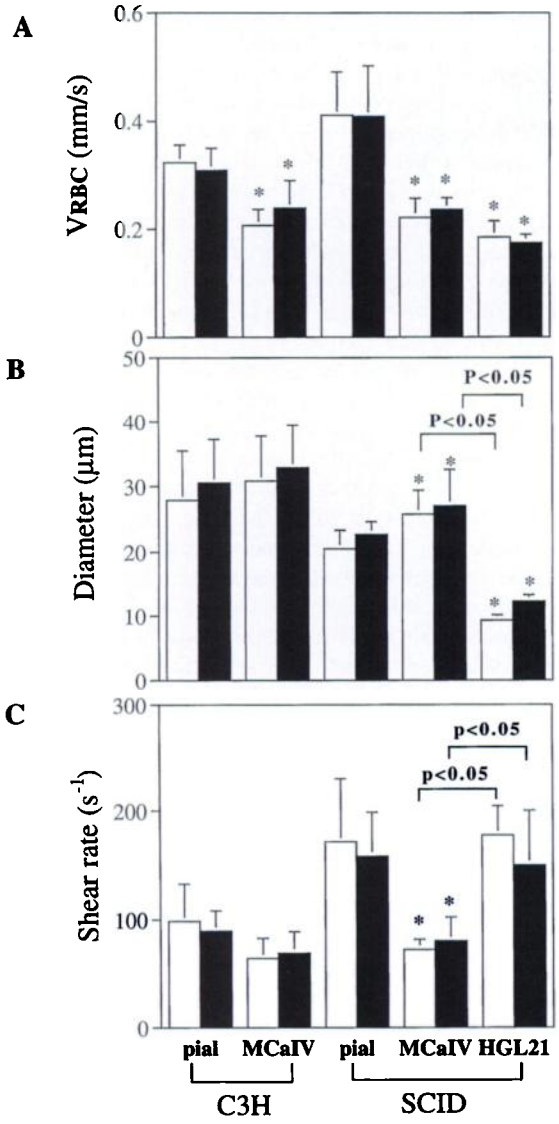

Fig. 3. Hemodynamic parameters in the cranial window. *A*, RBC velocity (*V*); *B*, vessel diameters (*D*); *C*, calculated shear rates by using *V* and *D* data in the cranial window. □, PBS treatment groups; ■, TNF-α treatment groups. *Columns*, mean; *bars*, SD. *, a statistically significant difference ($P < 0.05$) as compared with corresponding value of normal pial vessels.

promised, thus providing tumors with a mechanism for evasion of the host immune response. Measurement of the shear rates in the normal vessels of the skin and pial surface in C3H mice indicated that the hemodynamic forces acting against leukocyte rolling and adhesion were either comparable or less in the tumor vessels in these sites. Consequently, it is unlikely that the difference in number of rolling leukocytes between normal and tumor vessels was due to differences in the shear rate in the C3H mice. Two exceptions to this generalization were found with the MCaIV and HGL21 tumors grown in the cranial window of SCID mice, in which there was no significant difference between the basal rolling in the normal tissue and tumor tissue. In the case of the MCaIV tumor, the shear rates were significantly less than that in normal pial vessels, possibly promoting greater levels of rolling due to a more favorable hemodynamic environment. In the case of the HGL21 tumor in SCID mice, the combination of a relatively low frequency of rolling in the normal vessels when compared with the C3H pial vessels and a high variability of rolling frequency between animals could have obscured any differences in rolling that may exist.

Leukocyte rolling in both normal and tumor vessels was increased by TNF-α treatment, although not significantly in all cases. Because the shear rate was not altered by the TNF-α activation, it is unlikely that the frequency of leukocyte rolling was influenced by changes in the hemodynamic characteristics of the vessels. However, the increased rolling in the MCaIV tumor vessels in response to activation was significantly less than the response of the normal vessels in the skin, indicating that cytokine-mediated activation may not completely restore the ability of tumor vessels to support leukocyte rolling. This was not true for tumor vessels (both MCaIV and HGL21) in the cranial window. Rossler *et al.* (19) found that in brain tumors and inflammatory brain lesions, an up-regulation of endothelial ICAM-1 and LFA-3 expression was observed, whereas other adhesion molecules on endothelial cells remained unchanged. These findings suggest that the response to TNF-α may be attenuated to similar degrees in normal brain and tumor tissue in the same site.

In the interpretation of leukocyte adhesion observations, it is critical to consider the hemodynamic environment (8, 20). Although the

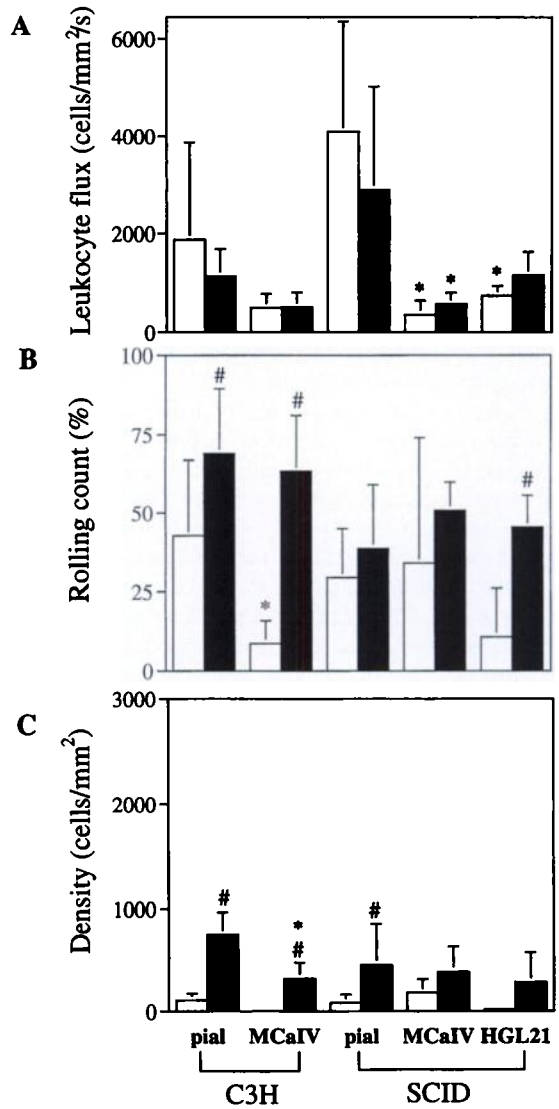

Fig. 4. Leukocyte-endothelial interaction in the cranial window. *A*, the normalized leukocyte flux; *B*, rolling count (100 × number of rolling cells/total number of cells) along 100-μm segment measuring for 30 s; *C*, density of binding cells. □, PBS treatment groups; ■, TNF-α treatment groups. *Columns*, mean; *bars*, SD. *, a statistically significant difference ($P < 0.05$) as compared with corresponding value of normal pial vessels. #, a statistically significant difference ($P < 0.05$) as compared with corresponding PBS control value.

Downloaded from http://aacrjournals.org/cancerres/article-pdf/55/21/4824/2459027/cr0550214824.pdf by guest on 24 August 2022

superfusion procedure did not alter the hemodynamics in the dorsal skin window, the RBC velocity in the cranial window significantly decreased after the coverslip was opened, and consequently, the level of leukocyte rolling was increased. Seki *et al.* (21) reported that the flow velocity of pial vessels in rat cranial window was significantly decreased after coverslip was opened and that this decrease was reversed by the restoration of intracranial pressure to 5 mm Hg. The value of the mean RBC velocity in this study, in same range diameter vessels, is comparable to our results. Our findings confirm that the removal of the cranial window may influence the hemodynamics and leukocyte-endothelial interaction. Attempts to introduce cytokines into the cranial window through ports and cannulas have proven technically difficult in the mouse model. For this reason, we chose the strategy of controlling for the hemodynamic changes with a mock control group and documenting the velocity changes.

Adhesion of leukocytes to normal and tumor vasculature without TNF-α activation was not significantly different and was very low in all cases. In response to TNF-α activation, the number of adherent cells increased significantly in both tumors. However, in the cranial window in SCID mice, it was not possible to demonstrate significant increases with either tumor, for the same reasons cited with regard to rolling, although the trend in these mice is suggestive of increased adhesion. Low leukocyte flux in tumors in cranial window could have affected these results.

MCaIV and HGL21 tumor vessels have different physiological properties, *i.e.*, vascular structure, hemodynamics, and permeability (16). The diameter of HGL21 tumor vessels was significantly smaller than that of MCaIV tumor, and as a result, the shear rate in HGL21 tumor vessels was significantly higher than in MCaIV in spite of comparable RBC velocity. This may be one reason why the basal leukocyte-endothelial interaction was generally higher in MCaIV than in HGL21. The relationship between flow rate and the numbers of interacting leukocytes is complex because higher levels of blood flow through a given vessel could potentially deliver a larger number of leukocytes/unit time; yet as the flow increases, the hemodynamic forces that displace cells from the endothelium also increase (20). As a result, this effect would be limited by the prohibitive shear rates, which are generated at high blood flow rates in small vessels, such as in the HGL21 tumor. This influence would be especially significant in vessels that have intrinsically lower levels of adhesion.

Although there is little direct evidence as yet to support a mechanism for the decreased leukocyte-endothelial interactions in tumor vessels, we suggest that one possible explanation may involve potential differences in the expression of selectins or integrin receptors on angiogenic vessels. In immunohistology studies of tumors, the majority of the staining for selectins and integrin receptors was associated with the normal tissue that surrounds the tumor but not with the tumor vessels (22). The majority of cellular infiltrates that are associated with tumors has been observed in the periphery of the tumor (23), suggesting that the cells have entered the tumor stroma from the normal tissue surrounding the tumor. Recently, Piali *et al.* (24) reported low expression of VCAM-1 on vessels in melanoma. In addition, both mRNA and protein levels of VCAM-1 in endothelioma cells were down-regulated by melanoma cells (24). In a contrasting study, the biopsies of human melanomas and renal cell carcinomas were found to have significant expression of VCAM-1, ICAM-1, and E-selectin (25). Immunostaining of endothelial cells isolated from murine tumors demonstrated increased expression of ICAM-2 (26). Jallal *et al.* (27) recently reported that expression of ICAM-1 and VCAM-1 in the tumor endothelium was significantly increased in 90K tumor-associated antigen-secreting tumor subsets in nude mice and expression levels of the 90K antigen in tumors inversely correlated with their tumorigenicity. However, heterogeneity of selectin and integrin expression in tumor vessels (24, 25) may result in overall decreased levels of leukocyte rolling and adhesion. Furthermore, tumor vessels with increased levels of adhesion molecules may be reduced or eliminated by the spontaneous cellular host response (27).

Another possible mechanism for the decreased leukocyte-endothelial interactions in tumors is low leukocyte flux in new angiogenic vessels. The results observed in the cranial window model support this possibility. Recent observations in basic fibroblast growth factor- or vascular endothelial growth factor-induced angiogenic vessels in collagen type I gel showed very low or no leukocyte flux.[4]

Observations of A-NK cell localization in tumor vasculature performed with adoptively transferred cell populations (12, 13, 28) and of localization of macrophage and NK cells in 90K antigen-secreting tumors (27) suggest that some circulating lymphocyte populations, such as NK cells, may have an increased capacity for adhesion to tumor vasculature. Consequently, IL-2-mediated activation of circulating NK populations could potentially result in a greater number of interacting cells within the tumor vessel. Such an effect could reconcile some of the differences observed in previous studies of leukocyte-endothelial interaction in tumor vessels (10, 11).

The ability to increase leukocyte interactions through the application of TNF-α directly on the tumor vasculature offers an opportunity to circumvent decreased leukocyte-endothelial interactions in tumor vessels, possibly through the production of cytokines by genetically modified lymphocyte or tumor cell populations. Because cytokine-mediated activation can be used to promote increased adhesion to tumor vasculature, this may present an effective strategy for increasing the number of cytotoxic effector cells that localize in the tumor vessels. Our current efforts are directed toward testing this concept.

Acknowledgments

We thank Drs. Herman D. Suit and Peigen Huang for providing the HGL21 tumor line, and Drs. Fan Yuan and Marc Dellian for helpful comments.

References

1. Hieber, U., and Heim, M. E. Tumor necrosis factor for the treatment of malignancies. Oncology (Basel), *51:* 142–153, 1994.
2. Fraker, D. L., Alexander, H. R., and Pass, H. I. Biologic therapy with TNF: systemic and regional administration. *In:* V. T. DeVita, S. Hellman, and S. A. Rosenberg (eds.), Biologic Therapy of Cancer, Ed. 2, pp. 62–69. Philadelphia: J. B. Lippincott Co., 1994.
3. Ostensen, M. E., Thiele, D. L., and Lipsky, P. E. Tumor necrosis factor-α enhances cytolytic activity of human natural killer cells. J. Immunol., *138:* 4185–4191, 1987.
4. Hallahan, D. E., Beckett, M. A., Kufe, D. W., and Weichselbaum, R. R. The interaction between recombinant tumor necrosis factor and radiation in 13 human tumor cell lines. Int. J. Radiat. Oncol. Biol. Phys., *19:* 69–74, 1990.
5. Weichselbaum, R. R., Hallahan, D. E., Beckett, M. A., Mauceri, H. J., Lee, H., Sukhatme, V. P., and Kufe, D. W. Gene therapy targeted by radiation preferentially radiosensitizes tumor cells. Cancer Res., *54:* 4266–4269, 1994.
6. Wong, G. H., McHugh, T., Weber, R., and Goeddel, D. V. Tumor necrosis factor alpha selectively sensitizes human immunodeficiency virus-infected cells to heat and radiation. Proc. Natl. Acad. Sci. USA, *88:* 4372–4376, 1991.
7. Folli, S., Pelegrin, A., Chalandon, Y., Yao, X., Buchegger, F., Lienard, D., Lejeune, F., and Mach, J. P. Tumor-necrosis factor can enhance radio-antibody uptake in human colon carcinoma xenografts by increasing vascular permeability. Int. J. Cancer, *53:* 829–836, 1993.
8. Melder, R. J., Munn, L. L., Yamada, S., Ohkubo, C., and Jain, R. K. Selectin and integrin mediated T lymphocyte rolling and arrest on TNFα-activated endothelium is augmented by erythrocytes. Biophys. J., in press, 1995.
9. Sluiter, W., Pietersma, A., Lamers, J. M., and Koster, J. F. Leukocyte adhesion molecules on the vascular endothelium: their role in the pathogenesis of cardiovascular disease and the mechanisms underlying their expression. J. Cardiovasc. Pharmacol., *22* (Suppl.)*:* S37–S44, 1993.
10. Wu, N. Z., Klitzman, B., Dodge, R., and Dewhirst, M. W. Diminished leukocyte-endothelium interaction in tumor microvessels. Cancer Res., *52:* 4265–4268, 1992.
11. Ohkubo, C., Bigos, D., and Jain, R. K. IL-2 induced leukocyte adhesion to the normal and tumor microvascular endothelium *in vivo* and its inhibition by dextran sulfate: implications for vascular-leak syndrome. Cancer Res., *51:* 1561–1563, 1991.

[4] M. Dellian, B. P. Witwer, H. A. Salehi, and R. K. Jain. Physiological characteristics of bFGF and VEGF/VPF induced microvessels: a novel assay for quantitation of angiogenesis in mice, submitted for publication.

Downloaded from http://aacrjournals.org/cancerres/article-pdf/55/21/4824/2459027/cr0550214824.pdf by guest on 24 August 2022

12. Sasaki, A., Melder, R. J., Whiteside, T. L., Herberman, R. B., and Jain, R. K. Preferential localization of human adherent lymphokine-activated killer (A-LAK) cells in tumor microcirculation. J. Natl. Cancer Inst., *83:* 433–437, 1991.
13. Melder, R. J., Brownell, A. L., Shoup, T. M., Brownell, G. L., and Jain, R. K. Imaging of activated natural killer cells in mice by positron emission tomography: preferential uptake in tumors. Cancer Res., *53:* 5867–5871, 1993.
14. Melder, R. J., Salehi, H. A., and Jain, R. K. Localization of activated natural killer cells in MCaIV mammary carcinoma grown in cranial windows in C3H mice. Microvasc. Res., *50:* 35–40, 1995.
15. Leunig, M., Yuan, F., Menger, M. D., Boucher, Y., Goetz, A. E., Messmer, K., and Jain, R. K. Angiogenesis, microvascular architecture, microhemodynamics, and interstitial fluid pressure during early growth of human adenocarcinoma LS174T in SCID mice. Cancer Res., *52:* 6553–6560, 1992.
16. Yuan, F., Salehi, H. A., Boucher, Y., Vasthare, U. S., Tuma, R. F., and Jain, R. K. Vascular permeability and microcirculation of gliomas and mammary carcinomas transplanted in rat and mouse cranial windows. Cancer Res., *54:* 4564–4568, 1994.
17. Villringer, A., Dirnagl, U., Them, A., Shurer, L., Krombach F., and Einhaul, K. M. Imaging of leukocytes within the rat brain cortex *in vivo*. Microvasc. Res., *42:* 305–315, 1991.
18. Atheron, A., and Born, G. V. R. Quantitative investigation of the adhesiveness of circulating polymorphonuclear leukocytes to blood vessel walls. J. Physiol., *222:* 447–474, 1972.
19. Rossler, K., Neuchrist, C., Kitz, K., Scheiner, O., Kraft, D., and Lassmann, H. Expression of leukocyte adhesion molecules at the human blood-brain barrier (BBB). J. Neurosci. Res., *31:* 365–374, 1992.
20. Perry, M. A., and Granger, D. N. Role of CD11/CD18 in shear rate-dependent leukocyte-endothelial cell interactions in cat mesenteric venules. J. Clin. Invest., *87:* 1798–1804, 1991.
21. Seki, J., Sasaki, Y., Oyama, T., and Yamamoto, J. Blood flow in pial microvessels in rats under open and closed cranial window preparations. *In:* H. Niimi, M. Oda, T. Sawada, and R. J. Xiu (eds.), Progress in Microcirculation Research, pp. 171–174. New York: Elsevier Science Publishing Co., Inc., 1994.
22. Kuzu, I., Bicknell, R., Fletcher, C. D., and Gatter, K. C. Expression of adhesion molecules on the endothelium of normal tissue vessels and vascular tumors. Lab. Invest., *69:* 322–328, 1993.
23. Dvorak, H. F., and Dvorak, A. Immunohistological characterization of inflammatory cells that infiltrate tumors. *In:* S. Haskill (ed.), Tumor Immunity in Prognosis: The Role of Mononuclear Cell Infiltration, pp. 279–307. New York: Marcel Dekker, Inc., 1982.
24. Piali, L., Fichtel, A., Terpe, H. J., Imhof, B. A., and Gisler, R. H. Endothelial vascular cell adhesion molecule 1 expression is suppressed by melanama and carcinoma. J. Exp. Med., *181:* 811–816, 1995.
25. Zocchi, M. R., and Poggi, A. Lymphocyte-endothelial cell adhesion molecules at the primary tumor site in human lung and renal cell carcinomas. J. Natl. Cancer Inst., *85:* 246–247, 1993.
26. Modzelewski, R. A., Davies, P., Watkins, S. C., Auerbach, R., Chang, M. J., and Johnson, C. S. Isolation and identification of fresh tumor-derived endothelial cells from a murine RIF-1 fibrosarcoma. Cancer Res., *54:* 336–339, 1994.
27. Jallal, B., Powell, J., Zachwieja J., Brakebusch, C., Germain, L., Jacobs, J., Iacobelli, S., and Ullrich, A. Suppression of tumor growth *in vivo* by local and systemic 90K level increase. Cancer Res., *55:* 3223–3227, 1995.
28. Basse, P. H., Nanmark, U., Johansson, B. R., Herberman, R. B., and Goldfarb, R. H. Establishment of cell-to cell contacts by adoptively transferred adherent lymphokine-activated killer cells with metastatic murine melanoma cells. J. Natl. Cancer Inst., *83:* 944–950, 1991.

Downloaded from http://aacrjournals.org/cancerres/article-pdf/55/21/4824/2459027/cr0550214824.pdf by guest on 24 August 2022